Applied Catalysis B: Environmental 165 (2015) 36–42

Contents lists available at ScienceDirect

Applied Catalysis B: Environmental

journal homepage: www.elsevier.com/locate/apcatb

A microwave-based method to monitor the ammonia loading of a vanadia-based SCR catalyst

Dieter Rauch [a,*], Gaby Albrecht [a], David Kubinski [b], Ralf Moos [a]

[a] Bayreuth Engine Research Center, Department of Functional Materials, University of Bayreuth, 95440 Bayreuth, Germany
[b] Ford Research and Advanced Engineering, 2101 Village Rd., Dearborn, Michigan 48124, USA

ARTICLE INFO

Article history:
Received 15 July 2014
Received in revised form
20 September 2014
Accepted 24 September 2014
Available online 2 October 2014

Keywords:
Selective catalytic reduction (SCR)
V_2O_5–WO_3/TiO_2
Ammonia storage
Microwaves.

ABSTRACT

For the selective catalytic reduction (SCR) of nitrogen oxides (NO_x) from lean burn diesel engines, NH_3 is used as reducing agent. In the case of V_2O_5–WO_3 catalysts supported on TiO_2 (anatase) ceramics, an adsorption of NH_3 on the catalyst surface is required for the SCR reactions. To effectively control the NH_3 supply and to obtain detailed knowledge on the catalyst status, it is crucial to know the current adsorbed amount of ammonia on the catalyst. It is shown for the first time in this study that it is possible to determine the ammonia loading of V_2O_5–WO_3 catalysts contactless and *in operando* by a simple microwave-based approach. This method can be applied for different temperatures. It is possible to determine the stored amount of ammonia independently on the ammonia-to-NO_x feed ratio.

1. Introduction

Increasing fuel costs and the pressure on automotive manufacturers from costumers and legislation to reduce CO_2 emissions lead to booming market shares for diesel engines. They are operated leanly. Nitrogen oxides (NO_x) cannot be removed with conventional three-way catalysts (TWCs), e.g. Ref. [1]. Therefore, novel exhaust gas after treatment concepts have emerged. For both heavy duty vehicles and passenger cars, selective ammonia catalytic reduction systems (NH_3-SCR) have already been serialized in the past few years [2]. In NH_3-SCR systems, an urea water solution (AdBlue™ or Diesel exhaust fluid, DEF) is injected into the exhaust. Ammonia is formed by hydrolysis and thermolysis. It serves as a selective reduction agent for NO_x, which is reduced to H_2O and N_2. The occurring reactions, with different reaction kinetics, depend on the NO-to-NO_2 ratio in the feed gas, according to Eqs. (1–3) [3].

$$4NH_3 + 4NO + O_2 \rightarrow 4N_2 + 6H_2O \quad (1)$$

$$4NH_3 + 2NO + 2NO_2 \rightarrow 4N_2 + 6H_2O \quad (2)$$

$$4NH_3 + 3NO_2 \rightarrow 7/2\,N_2 + 6H_2O \quad (3)$$

Eq. (1) is called the "standard" SCR reaction. The required oxygen is present in excess in typical diesel exhausts. When there are equimolar amounts of NO and NO_2 in the feed, the so-called "fast" SCR reaction [Eq. (2)] proceeds. This reaction is much faster than the "standard" reaction [4–6]. An oxidation catalyst is installed upstream of the SCR catalyst and the NH_3 injection valve. It enhances this reaction, since parts of the NO in the exhaust are converted to NO_2 [7]. Furthermore, such a pre-catalyst improves the overall performance because unburned hydrocarbons, which hinder the SCR process, are also oxidized [8]. Hence, it is difficult to adjust an NO_2 fraction of 50% as required for fast SCR, since the ambient conditions like space velocity and temperature of the exhaust change rapidly during transient automotive operation. Therefore, the oxidation is limited by the low-temperature activity of the pre-catalyst or by thermodynamics in the high temperature range [9]. In turn, the reaction with only NO_2 in the feed (Eq. (3), denoted "NO_2" SCR) is much slower than Eqs. (1 and 2), thus a NO:NO_2 ratio higher than 1:1 is not preferred [5,7,10].

Serial standard catalyst materials that are widely used for SCR in mobile applications are (besides zeolites) TiO_2 (anatase) supported V_2O_5–WO_3 (abbreviated in the following VWT) [11]. These materials show a high NO_x reduction performance in the temperature range from 300 to 500 °C [12,13]. At temperatures over 450 °C, unwanted side reactions, mainly NH_3 oxidation to NO and NO_2 [7,14], increase rapidly and limit the SCR activity [10,15–17]. The high temperature performance of these catalysts is also limited by anatase to rutile phase transformation of the Ti-support [10,18]

* Corresponding author at: Department of Functional Materials, University of Bayreuth, Universitätsstraße 30, 95440 Bayreuth, Germany. Tel.: +49 921557401; fax: +49 921557405.
E-mail address: funktionsmaterialien@uni-bayreuth.de (D. Rauch).

http://dx.doi.org/10.1016/j.apcatb.2014.09.059
0926-3373/

as well as the relative low melting point of V_2O_5 [16]. High temperature stability is of special importance, when the SCR catalyst is located downstream of a diesel particulate filter, because during filter regeneration, severe temperature peaks occur [13]. WO_3 acts as a stabilizer, as it hinders the anatase to rutile phase transformation of the support [12]. Moreover, it increases the SCR activity compared to binary V_2O_5/TiO_2 catalysts and limits sulfation [19,20]. The vanadium oxide species are the active sites in SCR catalysis. An increase of vanadium concentration enhances the NO_x reduction activity, but a high content leads to a loss of selectivity and thermal stability [10,21,22].

The SCR reaction mechanism over V_2O_5–WO_3/TiO_2 catalysts is reported to be based on an Eley-Rideal mechanism involving gaseous NO and adsorbed NH_3 [4,12,23–29]. NH_3 can adsorb on the catalyst surface on different sites, on Lewis as well as on Brønsted acidic sites [12,15,28,30]. The vanadium sites are the active sites for the SCR reactions [12,15,25,27,28,31]. Ti- and W-bound NH_3 species are strongly adsorbed but less reactive for SCR. Nevertheless, they are assumed to spill-over to reactive V-sites as soon as these become available during NH_3 consumption by NO_x. They serve as an NH_3 supply during SCR [12,15,24,25,27]. These mechanistic considerations point out that NH_3 adsorption on the catalyst surface is required for the SCR reactions to proceed.

Hence, to properly control the injection of the urea-water solution to obtain maximum NO_x conversion and minimum NH_3 slip, it is essential to know the current adsorbed amount of NH_3 on the catalyst. State-of-the-art for injection control are gas sensors up- and downstream of the catalyst in conjunction with raw emission models [32,33]. The microwave-based method presented in this study allows for detecting the ammonia loading directly and *in operando* without the deviation over the gas composition up- and downstream of the catalyst. It does not depend on modeled data. In this study, it is shown for the first time that it is possible to determine the ammonia loading of V_2O_5–WO_3 catalysts by a microwave-based approach.

2. Experimental setups and preliminary tests

All tests were performed in a laboratory test bench with synthetic exhaust. NO, NO_2, NH_3, O_2, and H_2O were balanced with N_2. The gas flows were controlled by mass flow controllers (MFCs, Brooks). All gas lines were heated over 185 °C to avoid condensation and formation of ammonium nitrate [5]. The downstream gas concentrations of H_2O, NH_3, NO, NO_2, and N_2O were monitored by a Fourier transformed infrared spectroscopy (FTIR) analyzer (Nicolet Antaris IGS) and O_2 by a wideband lambda probe (Bosch, LSU 4.9). The gas temperatures upstream and downstream of the catalyst were verified by type K thermocouples.

The catalyst examined in this study was an extruded serial type V_2O_5–WO_3/TiO_2 honeycomb monolith catalyst with a cell density of 300 cpsi. Extruded catalysts of this kind have been investigated thoroughly in literature, see e.g. Refs. [20,22,26].

Initial tests were performed in a quartz tube furnace. They were intended to generally characterize the catalyst with respect to conversion and to prove the functionality of the gas dosing unit of the test bench. A drill core of the extruded honeycomb device, of diameter 2.54 cm (1″) and length 5.08 cm (2″),was mounted in the quartz tube using glass wool as a sealant. A gas hourly space velocity (GHSV) of about 60,000 h^{-1} was applied (corresponding to a total gas flow of about 20 l min^{-1}). The feed ratio,

$$\alpha = \frac{c_{NH_3}}{c_{NO} + c_{NO_2}}, \quad (4)$$

was set to 0.9 with a total NO_x feed of 900 ppm. The background consisted of 7 % O_2 and 5 % H_2O, all balanced with N_2. The NO_x conversion was investigated as a function of temperature and feed gas composition in terms of NO_2-to-NO_x ratio. The results are shown in Fig. 1. In Fig. 1a, the NO_2 content in the feed with respect to the total NO_x concentration was increased from 0 to about 80 % at constant temperatures between 200 and 400 °C. As expected, the highest conversion occurs at all temperatures for $c_{NO} : c_{NO_2} = 1$, matching the "fast" SCR reaction condition [Eq. (2)]. With lower or higher NO_2 content, either the "standard" SCR reaction [Eq. (1)] or the "NO_2"-SCR reaction [Eq. (3)] predominate. Both are slower than the "fast" SCR reaction [4,5,10]. Therefore, the conversion decreases on both sides of the maximum. Furthermore, it can be seen that the conversion rate increases with increasing temperature. At the optimal NO_2 ratio of 50 %, the conversion at 300, 350 and 400 °C reaches 90 %, which is the maximum for $\alpha = 0.9$. The dependency on temperature can be seen even clearer in Fig. 1b. Here, the NO_x conversion is shown over temperature at constant NO_2/NO_x ratios. Again, the ratio of 50 % exhibits the highest conversion at all temperatures and the highest conversion appears once more in the temperature range between ~300 and ~400 °C. At lower temperatures, the chemical reactions are kinetically limited and at higher temperatures, unwanted side reactions, like NH_3 oxidation, occur [10,17]. Both effects yield a lower NO_x conversion. Nevertheless, even at 200 °C, a conversion rate of 55 % can be achieved if NO and NO_2 are in the feed gas in equimolar proportions. For higher NO_2 contents, the low temperature activity is even worse, as the "NO_2"-SCR reaction is the slowest one according to literature [5,10]. For real exhaust application, this behavior is not that important, since at higher temperatures, the thermodynamic equilibrium between

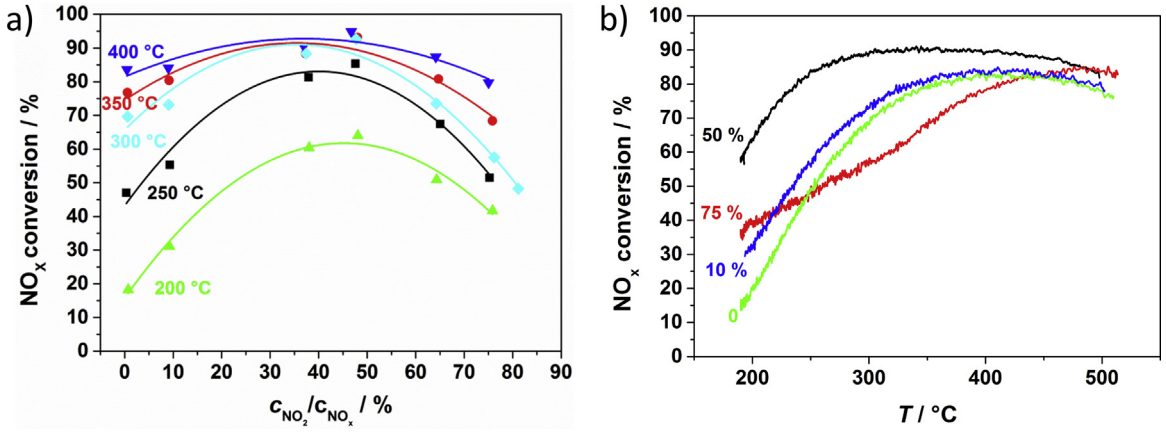

Fig. 1. NO_x conversion at a total NO_x feed of 900 ppm and a feed ratio of $\alpha = 0.9$ as a function of (a) the NO_2/NO_x ratio at different temperatures and (b) the temperature with varying NO_2 content.

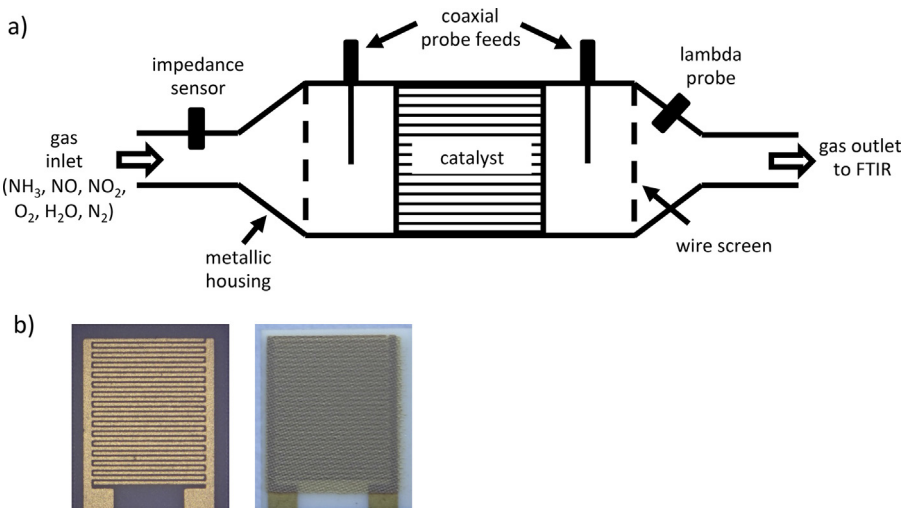

Fig. 2. Scheme of the experimental setup. (a) The metallic catalyst housing and the wire screens define an electromagnetic cavity resonator device; its microwave properties are determined by its geometry and the electrical properties of the catalyst monolith. (b) A sensor-like setup that allows determining the materials properties by impedance spectroscopy.

NO and NO_2 is on the NO side [10], promoting the "fast" SCR mechanism or the "standard" reaction, which becomes also fast at higher temperatures.

The microwave-based experiments were carried out using the same gas feed setup and the same analytics but a different reactor setup. For these tests, an extruded honeycomb structure catalyst sample, of diameter 6.03 cm (2 3/8″) and length 7.62 cm (3″), was mounted in a stainless steel canning utilizing glass wool for sealing. The canning was heated from the outside. For temperature monitoring, thermocouples were placed in the gas stream before and after the catalyst. A GHSV of about 11,000 h^{-1} was applied (corresponding to a total gas flow of about 40 l min^{-1}). As background gases, 7 % O_2 and 5 % H_2O balanced with N_2 were used for all tests. NH_3 and NO were admixed to the feed gas close to the catalyst with a sufficient distance for mixture. Measurements without honeycomb ensured that no gas conversion/oxidation on the hot parts of the metal canning occurred. To excite the electromagnetic waves, two coaxial probe feeds (electrically insulated stainless steel stubs) were mounted on the housing, one upstream and one downstream of the catalyst. The typical setup of the capacitive probe feeds is presented in Ref. [34]. This setup formed a two-port microwave network. To define the electrical length of the resonator, metallic wire screens were inserted at each end of the housing. They do not hinder the gas flow but prevent further propagation of the electromagnetic waves. The experimental setup is shown schematically in Fig. 2a.

The probe feeds were connected to a vector network analyzer (VNA, Anritsu MS 2025B) via coaxial cables. Using the network analyzer, the reflected and transmitted power over a defined frequency range can be detected. For these tests, the scattering parameters S_{ij} were measured in the frequency range from 1.7 to 6 GHz. They represent the ratios between the complex wave amplitude of the ingoing (a_j) and outgoing waves (b_i) where j denotes the ingoing port and i the outgoing port. Consequently, S_{11} is the reflection and S_{21} the transmission parameter. More details on the microwave-based technique for catalyst monitoring can be found in Refs. [35–38]. For the studies reported in this text, only the magnitude of the reflection parameter, $|S_{11}|$ (plotted in dB; $|S_{11}(f)|/\mathrm{dB} = 20 \cdot \log|S_{11}(f)|$) is considered.

For preliminary studies on the electrical properties of the catalyst material, an impedance sensor was placed upstream of the catalyst. As shown in Fig. 2b on the left, the sensor element consisted of an alumina substrate (Al_2O_3, 99.6% alumina), on which gold

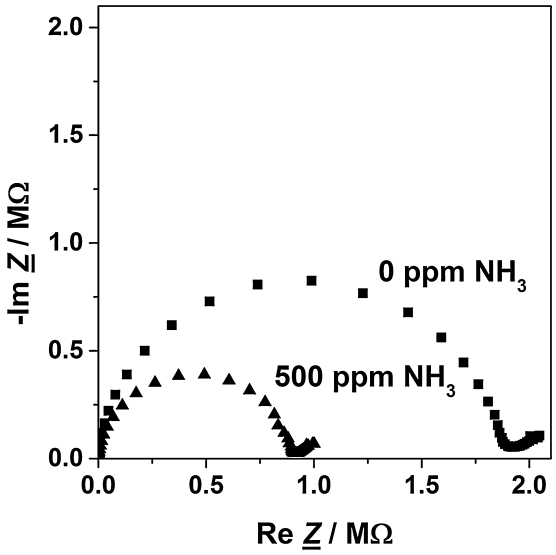

Fig. 3. Impedance spectra for 0 ppm and 500 ppm NH_3 in 7 % O_2 and 5 % H_2O at a sensor temperature of 300 °C.

interdigital electrodes were applied to form a planar interdigital capacitor with a line width and a line space of 100 μm. The electrodes were covered with a thick film of the SCR material as a sensitive layer (Fig. 2b right side). In order to do this, the extruded catalyst was crushed, sieved and mixed with an organic binder system. The obtained paste was screen-printed on the electrodes and fired at 600 °C. Such a sensor element was installed upstream of the catalyst (as shown in Fig. 2a) and was passively heated by the gas flow. Impedance spectra were taken by a Novocontrol Alpha-Analyzer in the frequency range of 1 Hz to 10 MHz with an amplitude of 50 mV.

Previous measurements on V_2O_5–WO_3/TiO_2 catalyst materials using electrical impedance spectroscopy [39] have shown that the material itself can be used as an ammonia sensor, as the sorbed NH_3 increases the conductivity of the material. Hence, the electric impedance signals correlate well with the NH_3 concentration in the gas. A corresponding increase in conductivity was found for the material under test in this study as well. In Fig. 3, the impedance spectra for 0 and 500 ppm NH_3 in 7 % O_2 and 5 % H_2O at 300 °C are shown in a Nyquist plot. Each spectrum consists of a semicircular

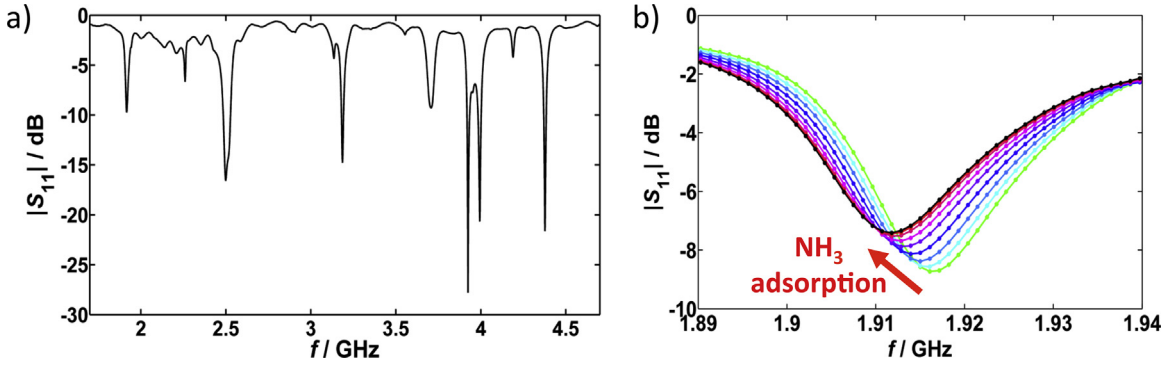

Fig. 4. (a) Frequency spectrum of S_{11} in background gas at 300 °C and (b) first resonance mode of S_{11} during exposure to 500 ppm NH_3, recorded in an interval of about 2 min (green curve: without NH_3, black curve: catalyst saturated with NH_3).

shape in the high frequency region, which represents the material properties, and a tail in the low frequency region, originating from the electrode interfaces [39]. By applying an $R||C$ equivalent circuit, the diameter represents the resistance of the material. In presence of NH_3, the diameter of the semicircle decreases, indicating that the impedance decreases due to ammonia adsorption. During the tests below, the sensor was measured at a constant frequency and the magnitude of the complex impedance $|Z|$ was evaluated as a measure for the ammonia loading of the sensing device.

In order to monitor the changing electrical properties due to NH_3 exposure on the honeycomb structure catalyst by using the microwave-based method, the magnitudes of the scattering parameters obtained from the network analyzer are plotted over frequency. The spectrum of $|S_{11}|$ for the ammonia-unloaded catalyst at 300 °C in background gas (7 % O_2 and 5 % H_2O in N_2) is shown in Fig. 4a. As can be seen, at discrete frequencies, peaks occur in the microwave signal. At these frequencies, standing electromagnetic waves, the so-called resonance modes, form in the resonator. Their frequencies, the resonance frequencies f_{res}, depend on the electrical properties of the resonator filling. This has been extensively shown for three-way catalysts [40,41], for lean NO_x traps [42,43], for diesel particulate filters [44,45] and for a zeolite-based SCR catalyst [46]. As the conductivity of the catalyst material increases due to the adsorption of ammonia (see Fig. 3), the electric losses increase, whereby the propagation of the electromagnetic waves is affected. The perturbation of the electric and magnetic field associated with the NH_3 loading can be monitored by a shift of the resonance frequencies to lower values and a decrease of the peak depth. In Fig. 4b, the first resonance mode, namely the TE_{111} mode, of the spectrum of $|S_{11}|$ is magnified. The green curve was recorded in the absence of ammonia. Thereafter, the catalyst was exposed to 500 ppm NH_3. The further curves were captured in an interval of about 2 min. With increasing exposure time and subsequently a higher adsorbed amount of NH_3, the peak shifted to lower frequencies by 4.9 MHz and the depth was decreasing, until the catalyst was saturated (black curve). The resonance frequency shift, as it depends on the adsorption of ammonia, can be utilized to monitor the NH_3 loading of the vanadia-doped tungsten-titania catalyst appropriately.

3. Results and discussion

The capability of the microwave-based method to determine the NH_3 adsorption on the vanadia-doped tungsten-titania catalyst was investigated with different ammonia concentrations and various feed ratios at temperatures between 200 and 400 °C in this study. As signal characteristic, the resonance frequency of the TE_{111} mode in the spectrum of the reflection parameter S_{11} was monitored over time in all tests. In Fig. 5, a storage measurement

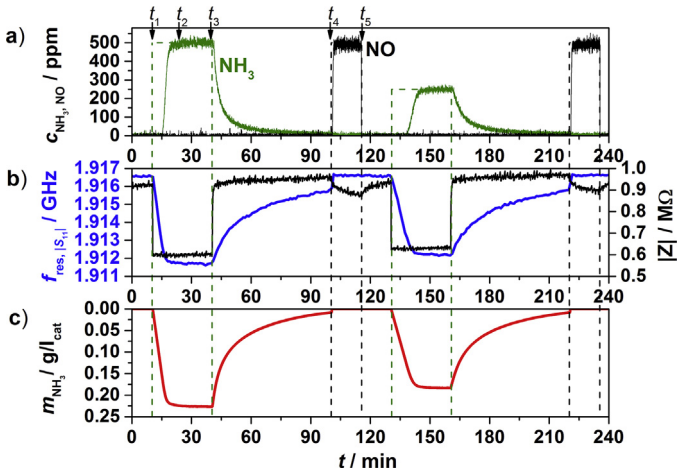

Fig. 5. Storage measurement at 300 °C. (a) Inlet (dashed lines) and outlet (solid lines) gas concentrations of NH_3 (green) and NO (black), (b) resonance frequency (blue) and impedance sensor signal (black) and c) calculated amount of NH_3 stored on the catalyst.

at 300 °C in background gas (7 % O_2 and 5 % H_2O in N_2) is depicted. In this test, an impedance sensor was mounted upstream of the catalyst. Figure 5a shows the inlet and outlet gas concentrations of NH_3 and NO over time. The dashed lines indicate the inlet concentrations (derived from MFC output data) and the solid lines are the gas concentrations measured by FTIR downstream of the catalyst. In Fig. 5b, the resonance frequency is plotted in blue and the magnitude of the complex impedance of the sensor element, measured at a constant frequency of 20 Hz, in black.

As can be seen, in the beginning of the measurement ($t = 0$), only O_2 and H_2O were fed. Resonance frequency and sensor signal remained on a constant level. After 10 min (t_1), 500 ppm NH_3 were admixed to the gas flow. The sensor impedance $|Z|$ dropped immediately by about 320 kΩ and remained constant afterwards. Because the sensor was placed upstream of the catalyst, it was loaded promptly with NH_3 due to the small dimensions of its functional layer compared to the large amount of ammonia it was exposed to. The resonance frequency (f_{res}) was also decreasing when NH_3 was admixed due to ammonia sorption on the honeycomb catalyst. The resonance frequency decreased by far slower than the impedance, since the volume of the catalyst was much bigger and therefore provided a higher storage capacity. For the first 5 min of NH_3 dosing, all ammonia was stored on the catalyst, indicated by zero NH_3 detected by FTIR downstream of the catalyst. During this period, f_{res} was decreasing linearly. At about 16 min (t_2), NH_3 started to break through and the downstream concentration was increasing until it reached the inlet value of 500 ppm. At this

point of time, the catalyst was fully saturated with ammonia. As soon as there was no more storage, the resonance frequency also reached a final value, which is a measure for the catalyst ammonia loading level. At 40 min (t_3), ammonia was turned off and the downstream concentration was slowly decreasing, due to NH_3 desorption from the acid storages sites. This desorption went along with an increase of the resonance frequency. Desorption of ammonia stored on the impedance sensor was more rapid because of the high space velocity. Thus, it took only 2 min after NH_3 shutoff until the impedance was back on its unloaded value of 920 kΩ. After 100 min (t_4), the ammonia concentration downstream of the catalyst was lower than 15 ppm, indicating that desorption was almost completed. At the same time, the resonance frequency attained an almost constant level, but below the unloaded value, indicating that some NH_3 was still left on the catalyst. Therefore, 500 ppm NO were added to the gas to convert the remaining NH_3 on the catalyst by the "standard" SCR reaction according to Eq. (1). It took about 3 min until the NO inlet concentration was detected downstream of the catalyst. During this period, the remaining NH_3 on the catalyst was converted by NO to N_2 and H_2O and the resonance frequency was quickly returning to its unloaded value. Both, the NO concentration and the resonance frequency illustrate that the catalyst was completely unloaded again. The impedance sensor shows a slight cross sensitivity to NO as the impedance value was decreasing during NO dosing and instantly recovering after NO was turned off after 115 min (t_5), a behavior that has been reported previously [47].

Subsequently, the same test procedure was repeated with an inlet concentration of 250 ppm NH_3. The lower feed concentration resulted in a 4 min longer period of time required for catalyst ammonia saturation, compared to the loading with 500 ppm. It was accompanied by a slower decrease of the resonance frequency. Also, the change of f_{res} due to loading was lower than before. The impedance was again dropping immediately when NH_3 was turned on, but the change in signal was also lower than in the former case. Both desorption and response to NO admixture showed the same characteristics as in the first test.

To compare both storage procedures, the stored amount of ammonia was calculated by balancing and integration of inlet and outlet gas concentrations [Eq. (5)].

$$m_{NH_3} = \rho_{NH_3}\dot{V} \cdot \int \left(c_{NH_3,in} - c_{NO,in} - c_{NH_3,FTIR} + c_{NO,FTIR}\right) dt. \quad (5)$$

In Eq. (5), m_{NH_3} stands for the stored ammonia mass on the catalyst, ρ_{NH_3} is the density of ammonia, and $\dot{V}$ the volumetric gas flow. c_{in} are the MFC output data for NH_3 and NO and c_{FTIR} the gas concentrations measured downstream of the catalyst. The stored mass of ammonia per liter catalyst volume as calculated from Eq. (5) is plotted in Fig. 5c. It must be noted that a reverse scaling is used for better comparability. It comes to 226 mg per liter catalyst volume for loading with 500 ppm and 183 mg per liter for 250 ppm NH_3 when the catalyst is saturated. This plot shows even more clearly the outstanding correlation between the resonance frequency and the stored amount of ammonia during storage as well as desorption and conversion with NO. Also, it can be seen that in the case of an inlet of 250 ppm NH_3, the stored amount was lower, resulting in a smaller change in f_{res}.

To emphasize the correlation between the degree of ammonia loading and the response of the microwave signal, the shift of the resonance frequency of the TE_{111} mode during loading with 500 ppm NH_3 is plotted over the calculated amount of NH_3 stored on the catalyst in Fig. 6 for measurements at 200, 300 and 400 °C. Starting in the unloaded state (upper left of the plot), f_{res} decreases due to adsorption of NH_3 until the catalyst was saturated (right end of the curves). Accordingly, the curve for 300 °C corresponds to the time period between t_2 and t_3 in Fig. 5. At 400 °C, ammonia

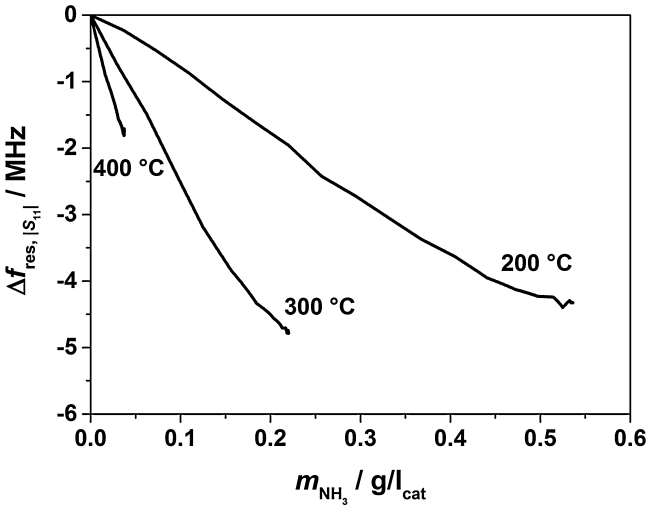

Fig. 6. Resonance frequency shift over calculated amount of NH_3 stored on the catalyst for 200, 300 and 400 °C.

was partially oxidized to N_2 and H_2O over the catalyst [17], so that the downstream gas concentration of NH_3 only reached 310 ppm when saturated with 500 ppm NH_3. For the calculation of the stored amount, this value was taken into account, presuming that the oxidation took place before storage.

One clearly can see that there is an almost linear relationship between the change in resonance frequency and the amount of ammonia on the catalyst. With increasing temperature, the amount of stored NH_3 decreases because the storage capacity lowers [15,25]. So, the amount on saturation decreases from 536 mg l_{cat}^{-1} at 200°C to 220 mg l_{cat}^{-1} at 300°C and further to 37 mg l_{cat}^{-1} at 400°C. Evaluating the slopes of the curves reveals the sensitivity of the microwave-based method in MHz to the amount of NH_3 stored on the catalyst referred to the catalyst volume (MHz $g_{NH_3}^{-1}$ l_{cat}^{-1}). In contrast to the stored amount, the sensitivity increases with increasing temperature. For 200°C, it amounts to 8.5 MHz $g_{NH_3}^{-1}$ l_{cat}^{-1}. For 300°C, it raises to about 22.5 MHz $g_{NH_3}^{-1}$ l_{cat}^{-1} and for 400°C to 48.3 MHz $g_{NH_3}^{-1}$ l_{cat}^{-1}. Using these parameters, it is possible to calculate the stored amount of NH_3 based on the frequency shift at the measured temperatures. Linear regression of the sensitivity values furthermore allows for determining the stored amount using the shift of f_{res} at other temperatures. The reason for the temperature dependence of the sensitivity is assumed to be that ammonia is adsorbed on different sites on the catalyst, e.g. Lewis and Brønsted acid sites as well as Ti- and W-bound ammonia [12,15], depending on temperature. These sites might contribute in different ways to the electrical properties of the catalyst material and therefore are detected by the microwave-based method in different extent. The active material V_2O_5 is an n-type semiconductor [48]. The main charge carriers are electrons generated by oxygen vacancies in the lattice of non-stoichiometric V_2O_5 [49]. The charge carrier density depends on the surrounding gas atmosphere. In presence of reducing gases, adsorbed oxygen ions react with the reducing species. This reduces the surface vanadate layer (V^{5+} to V^{4+}) and a conduction electron is released as an additional oxygen vacancy is created [50]. It is suggested that the electrons can hop between vanadium ions in different valence states [51]. Such surface reactions are the main sensing principle for all n-type conducting metal oxide semiconducting gas sensors when exposed to reducing gases [52], in contrast to zeolite-based SCR catalysts, where the adsorption of NH_3 causes an increase in the proton conductivity of the material [53]. NH_3 is assumed to adsorb on the V_2O_5 surface at hydroxyl V–OH sites (Brønsted acid centers) as

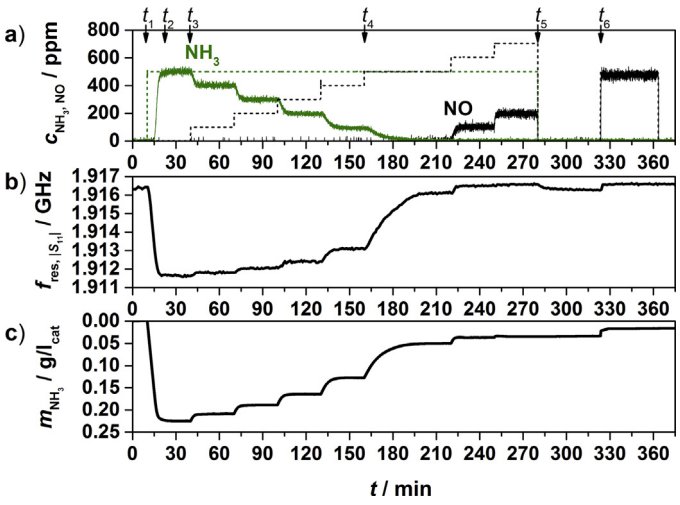

Fig. 7. Storage measurement with varying feed ratio at 300 °C. (a) Inlet (dashed) and outlet (solid) concentrations of NH_3 (green) and NO (black), (b) resonance frequency and (c) calculated amount of NH_3 stored on the catalyst.

NH^{4+} cation [54–57]. As a consequence, vanadia is reduced and thereby the charge carrier density increases [51]. Thus, the electrical conductivity increases in the presence of ammonia and can be detected by the microwave technique. Additionally, it was recently corroborated by Heine et al. that it is possible to measure at microwave frequencies the increase of the conductivity of V_2O_5 by applying reducing gases [58]. They performed microwave cavity perturbation measurements on a α-V_2O_5 powder at 9.2 GHz. By applying n-butane as reducing gas, these authors monitored an increase in the electrical conductivity based on the aforementioned theory. Beyond these considerations, one has to keep in mind that in the VWT composition, two more semiconducting materials, WO_3 and TiO_2, are involved. NH_3 can adsorb on these materials as well [15] and therefore, these oxides could contribute to the conductivity as well. In this study, with increasing temperature, the adsorbed amount of ammonia decreases together with a decrease of the conductivity, but to a larger extent. Thus, it is not clear yet which mechanism is predominant for the vanadia-based catalyst investigated. These considerations about the mechanism of action have to be evaluated in more detail in future work. Nevertheless, it is possible to develop characteristic lines for the stored amount at given temperatures so far.

To examine the capability of the presented microwave-based method under SCR conditions, tests with different feed ratios have been performed. At first, the catalyst was saturated with ammonia ($\alpha = \infty$) and then the NO concentration was stepwise increased by 100 ppm up to a feed ratio of about $\alpha \approx 0.7$ (500 ppm NH_3/700 ppm NO). Figure 7 shows an experiment of that kind at 300 °C. In Fig. 7a, the gas concentrations of NH_3 and NO of inlet (MFC, dashed curve) and outlet (FTIR, solid curve) are illustrated. Figure 7b shows the resonance frequency of the TE_{111} mode and Fig. 7c the calculated amount of stored ammonia in reversed scaling for comparison.

At the beginning, the catalyst was unloaded and the resonance frequency remained at 1.9163 GHz. After 10 min (t_1) in background gas, 500 ppm NH_3 were admixed to the gas flow and the catalyst was instantaneously storing all the incoming ammonia, indicated by the fact that no NH_3 occurred downstream of the catalyst. The adsorption was accompanied by a linear decrease of the resonance frequency according to the increase in the calculated stored amount of NH_3. After 22 min (t_2), the inlet concentration of 500 ppm NH_3 was detected in the outlet, indicating that the catalyst was fully loaded, and the stored amount of NH_3 accounted to 225 mg l_{cat}^{-1}. At the same time, f_{res} reached a constant value of 1.9116 GHz. After 40 min (t_3), 100 ppm NO were added. All the NO was converted by the "standard" SCR reaction [Eq. (1)], consuming the same stoichiometric amount of NH_3, as can be seen by the decrease of the ammonia concentration to 400 ppm. Even so, it took about 5 min for the ammonia concentration to reach this level. During this period of time, part of the stored ammonia was used for NO conversion, indicated by a slight increase of the resonance frequency and a decrease of the calculated stored amount. In an interval of 30 min, the NO concentration was increased further by steps of 100 ppm. Up to the level with a feed ratio of 1 ($c_{NH_3,in} = c_{NO,in}$) in the inlet gas, the NH_3 concentration was decreased stepwise by the amount of added NO with an initial consumption of stored NH_3. This was monitored by the resonance frequency as well. After 160 min (t_4), equal amounts of both reaction gases were added to the feed. This is the point where the catalyst is optimally operated. In this step, it took about 37 min until the NO diminished downstream of the catalyst. This implies that a large part of the stored NH_3 was consumed, as can be seen by an extensive decrease in the stored amount and a large increase of the resonance frequency. As soon as the concentrations of NH_3 and NO came to zero in the outlet, indicating that there is no more consumption of stored ammonia, f_{res} remained on a constant level. By increasing the NO concentration further, there was only low consumption of stored NH_3, resulting in a minor change in the resonance frequency and NO was detected by the FTIR. Even in excess of 200 ppm NO, there ought to be some NH_3 stored on the catalyst, as it is mandatory for the SCR reaction to occur [12]. This precondition cannot fully be proven by the microwave-based technique, as the resonance frequency went already back to its unloaded value. Probably, the amount of adsorbed NH_3 is too small to be certainly detected. After 280 min (t_5), NH_3 and NO were turned off and instantly, f_{res} was slightly decreasing. A possible reason therefore is that the adsorbed NH_3 is migrating to a storage site which is more sensitive to the microwave-based method when only dosing H_2O and O_2. It is proposed in literature that on a V_2O_5–WO_3/TiO_2 catalyst a differentiation has to be made between NH_3 reaction and NH_3 adsorption sites [25,27]. In future work, it has to be determined the adsorption of which sites are detected by the microwave-based method. After 324 min (t_6), 500 ppm NO were added and an instantaneous increase in resonance frequency and a decrease in the stored amount occurred, suggesting that the remaining NH_3 on the catalyst is eventually converted. This cannot be evidenced by FTIR as the consumed amount of NO is quite small and is in the range of the response time of the FTIR owed to the gas pathways. The fact that the calculated amount of NH_3 does not come back to zero may be due to integration errors and measuring inaccuracies. Nevertheless, a clear correlation between the shift of the resonance frequency and the stored amount of NH_3 can be recognized under SCR conditions as well.

4. Conclusions

In this work, a recent technique was successfully applied to detect directly and *in operando* the ammonia loading of the oxide-based SCR catalyst of V_2O_5–WO_3/TiO_2. For that purpose, microwaves were excited in the metallic catalyst housing and their resonance frequencies were tracked during loading of the catalyst with different NH_3 concentrations and feed ratios at multiple temperatures. A linear correlation was found between the microwave signal and the mass of stored ammonia on the catalyst during loading. Under more realistic conditions with a varying NO concentration in the feed gas, a very good correlation was found between the resonance frequency and the current amount of NH_3 adsorbed on the catalyst. In future work, the microwave-based results will be correlated with ammonia adsorption isotherms. For this purpose, a special setup has been established recently, which

allows measuring small powder samples directly under reaction conditions [59]. With this setup, the complex dielectric constant (permittivity and losses) can be determined by comparing the resonance spectra with a defined reference. This will also help to fully clarify the origin of the resonance frequency shift with ammonia adsorption. From just looking on the resonance frequency one cannot exclude that a permittivity increase due to a higher polarizability is responsible for the effect. The results in Ref. [59] indicated that in H-ZSM-5 zeolites, both permittivity and losses contribute to the resonance frequency shift that occurs when ammonia is sorbed. However, even losses can originate from two different effects, since one has to differentiate between contributions from electronic conductivity (as assumed above) and from dielectric losses.

Acknowledgements

We thank Johnson Matthey (Germany) GmbH for providing the catalyst sample.

References

[1] M. Shelef, R.W. McCabe, Catal. Today 62 (2000) 35–50.
[2] T.V. Johnson, Int. J. Eng. Res. 10 (2009) 275–285.
[3] W. Weisweiler, Chem. Ing. Tech. 72 (2000) 441–449.
[4] I. Nova, C. Ciardelli, E. Tronconi, D. Chatterjee, B. Bandl-Konrad, Catal. Today 114 (2006) 3–12.
[5] M. Koebel, G. Madia, M. Elsener, Catal. Today 73 (2002) 239–247.
[6] M. Koebel, G. Madia, F. Raimondi, A. Wokaun, J. Catal. 209 (2002) 159–165.
[7] M. Koebel, M. Elsener, G. Madia, Ind. Eng. Chem. Res. 40 (2001) 52–59.
[8] G. Madia, M. Koebel, M. Elsener, A. Wokaun, Ind. Eng. Chem. Res. 41 (2002) 3512–3517.
[9] M. Iwasaki, H. Shinjoh, Appl. Catal. A: General 390 (2010) 71–77.
[10] M. Koebel, M. Elsener, M. Kleemann, Catal. Today 59 (2000) 335–345.
[11] O. Deutschmann, J.-D. Grunwaldt, Chem. Ing. Tech. 85 (2013) 1–24.
[12] G. Busca, L. Lietti, G. Ramis, F. Berti, Appl. Catal. B: Env. 18 (1998) 1–36.
[13] B. Guan, R. Zhan, H. Lin, Z. Huang, Appl. Therm. Eng. 66 (2014) 395–414.
[14] G. Madia, M. Koebel, M. Elsener, A. Wokaun, Ind. Eng. Chem. Res. 41 (2002) 4008–4015.
[15] M. Kleemann, M. Elsener, M. Koebel, A. Wokaun, Appl. Catal. B: Env. 27 (2000) 231–242.
[16] O. Kroecher, M. Elsener, Ind. Eng. Chem. Res. 47 (2008) 8588–8593.
[17] C. Ciardelli, I. Nova, E. Tronconi, B. Konrad, D. Chatterjee, K. Ecke, M. Weibel, Chem. Eng. Sci. 59 (2004) 5301–5309.
[18] A. Grossale, I. Nova, E. Tronconi, D. Chatterjee, M. Weibel, J. Catal. 256 (2008) 312–322.
[19] B.W. Lee, H. Cho, D.W. Shin, J. Ceram. Process. Res. 8 (2007) 203–207.
[20] L. Lietti, J.L. Alemany, P. Forzatti, G. Busca, G. Ramis, E. Giamello, F. Bregani, Catal. Today 29 (1996) 143–148.
[21] G. Madia, M. Elsener, M. Koebel, F. Raimondi, A. Wokaun, Appl. Catal. B: Env. 39 (2002) 181–190.
[22] S. Djerad, L. Tifouti, M. Crocoll, W. Weisweiler, J. Mol. Catal. A: Chem. 208 (2004) 257–265.
[23] M. Koebel, M. Elsener, Chem. Eng. Sci. 53 (1998) 657–669.
[24] L. Lietti, I. Nova, S. Camurri, E. Tronconi, P. Fortatti, AIChE J. 43 (1997) 2559–2570.
[25] L. Lietti, I. Nova, E. Tronconi, P. Forzatti, Catal. Today 45 (1998) 85–92.
[26] I. Nova, L. Lietti, E. Tronconi, O. Forzatti, Catal. Today 60 (2000) 73–82.
[27] I. Nova, L. Lietti, E. Tronconi, P. Forzatti, Chem. Eng. Sci. 56 (2001) 1229–1237.
[28] J.A. Dumesic, N.-Y. Topsøe, Y. Chen, T. Slabiak, J. Catal. 163 (1996) 409–417.
[29] E. Tronconi, I. Nova, C. Ciardelli, D. Chatterjee, M. Weibel, J. Catal. 245 (2007) 1–10.
[30] T.Z. Srnak, J.A. Dumesic, B.S. Clausen, E. Toernqvist, N.-Y. Topsøe, J. Catal. 135 (1992) 246–262.
[31] N.-Y. Topsøe, J.A. Dumesic, H. Topsøe, J. Catal. 151 (1995) 241–252.
[32] F. Willems, R. Cloudt, E. van den Eijnden, M. van Genderen, R. Verbeek, B. de Jager, W. Boomsma, I. van den Heuvel, SAE Technical Paper 2007-01-1574 (2007).
[33] D.Y. Wang, S. Yao, M. Shost, J.-H. Yoo, D. Cabush, D. Racine, R. Cloudt, F. Willems, SAE International Journal of Passenger Cars - Electronic and Electrical Systems 1 (2009) 323–333.
[34] D. Rauch, P. Fremerey, A. Jess, R. Moos, Sens. Actuators B: Chem. 181 (2013) 681–689.
[35] G. Fischerauer, M. Spörl, A. Gollwitzer, M. Wedemann, R. Moos, Frequenz 62 (2008) 180–184.
[36] R. Moos, M. Spörl, G. Hagen, A. Gollwitzer, M. Wedemann, G. Fischerauer, SAE Technical Paper 2008-01-0916 (2008).
[37] R. Moos, G. Beulertz, S. Reiß, G. Hagen, G. Fischerauer, M. Votsmeier, J. Gieshoff, Top. Catal. 56 (2013) 358–364.
[38] R. Moos, G. Fischerauer, Oil Gas Sci. Technol. – Rev., IFP Energies nouvelles, Rueil-Malmaison, 2014, http://dx.doi.org/10.2516/ogst/2013203, in press.
[39] D. Schönauer, I. Sichert, R. Moos, Sens. Actuators B: Chem. 155 (2011) 199–205.
[40] S. Reiß, M. Spörl, G. Hagen, G. Fischerauer, R. Moos, IEEE Sens. J. 11 (2011) 434–438.
[41] G. Beulertz, M. Fritsch, G. Fischerauer, F. Herbst, J. Gieshoff, M. Votsmeier, G. Hagen, R. Moos, Top. Catal. 56 (2013) 405–409.
[42] P. Fremerey, S. Reiß, A. Geupel, G. Fischerauer, R. Moos, Sensors 11 (2011) 8261–8280.
[43] R. Moos, M. Wedemann, M. Spörl, S. Reiß, G. Fischerauer, Top. Catal. 52 (2009) 2035–2040.
[44] M. Feulner, G. Hagen, A. Piontkowski, A. Müller, G. Fischerauer, D. Brüggemann, R. Moos, Top. Catal. 56 (2013) 483–488.
[45] G. Fischerauer, M. Förster, R. Moos, Meas. Sci. Technol. 21 (2010) 035108.
[46] S. Reiß, D. Schönauer, G. Hagen, G. Fischerauer, R. Moos, Chem. Eng. Technol. 34 (2011) 791–796.
[47] R. Moos, R. Müller, C. Plog, A. Knezevic, H. Leye, E. Irion, T. Braun, K.-J. Marquardt, K. Binder, Sens. Actuators B: Chem. 83 (2002) 181–189.
[48] J. Goclon, R. Grybos, M. Witko, J. Hafner, Phys. Rev. B 79 (2009) 075439.
[49] O. Schilling, K. Colbow, Sens. Actuators B 21 (1994) 151–157.
[50] J.-M. Herrmann, J. Disdier, Catal. Today 56 (2000) 389–401.
[51] R.B. Bjorklund, C.U.I. Odenbrand, J.G.M. Brandin, L.A.H. Andersson, B. Liedberg, J. Catal. 119 (1989) 187–200.
[52] R. Moos, K. Sahner, M. Fleischer, U. Guth, N. Barsan, U. Weimar, Sensors 9 (2009) 4323–4365.
[53] M.E. Franke, U. Simon, ChemPhysChem 5 (2004) 465–472.
[54] M. Inomata, A. Miyamoto, Y. Murakami, J. Catal. 62 (1980) 140–148.
[55] M. Gasior, J. Haber, T. Machjzj, T. Czeppe, J. Mol. Catal. 43 (1988) 359–369.
[56] S. Surnev, M.G. Ramsey, F.P. Netzer, Prog. Surf. Sci. 73 (2003) 117–165.
[57] M. Szaleniec, A. Drzewiecka-Matuszek, M. Witko, P. Hejduk, J. Mol. Model. 19 (2013) 4487–4501.
[58] C. Heine, F. Girgsdies, A. Trunschke, R. Schlögl, M. Eichelbaum, Appl. Phys. A 112 (2013) 289–296.
[59] M. Dietrich, D. Rauch, A. Porch, R. Moos, Sensors 14 (2014) 16856–16868.